Journal of Information Systems Engineering and Management
2025, 10(35s)
e-ISSN: 2468-4376
https://www.jisem-journal.com/

Research Article

Coati Optimization Based PID Controller for Stability Analysis of Micro Grid with Photo Voltaic Distributed Generator

Muhamad Nabil Bin Hidayat[1], Naeem Hannoon*[2], Anshuman Satapathy[3], Dalina Binti Johari[4]
[1,2,4]*School of Electrical Engineering, College of Engineering, Universiti Teknologi Mara, Shah Alam, Malaysia.*
[3]*Department of EEE, ITER, SOA Deemed to be University, Odisha, India*

ARTICLE INFO

Received: 18 Dec 2024
Revised: 10 Feb 2025
Accepted: 28 Feb 2025

ABSTRACT

This study investigated system stability in a multi-source micro grid incorporating photo voltaic energy sources. The primary objective was to maintain system parameters for sustainable power supply. A Proportional Integral Derivative (PID) controller was implemented as a secondary controller to regulate micro grid parameters during grid connected mode operations. The performance index used was the integral of squared error (ISE). To enhance the optimization process for nonlinear controller design, coati Optimization algorithm (COA), an advanced Optimization method, was employed. The micro grid under test included distributed generation units such as two photovoltaic systems. Results demonstrated that the proposed controller effectively performed during various operating conditions, achieving desired responses swiftly while enhancing stability and reducing oscillations compared to conventional methods. Coati optimization based PID controller shows a significant advancement in ensuring efficient stability approach in micro grids with multiple renewable energy sources, thereby contributing to improved system reliability and performance. The proposed techniques quickly damped out the oscillations as compared to conventional controllers.

Keywords: Coati Optimization Algorithm, PID Controller., VSC controller, Grid stability

INTRODUCTION

The increasing electricity demand forecasts have spurred global efforts towards deploying cost-effective and environmentally sustainable Renewable Energy Sources (RES). This shift from conventional methods to RES for power generation has catalysed the emergence of micro grids, aimed at distributing generation and partially relieving loads from the interconnected power grid. A micro grid (MG) consists of multiple small-scale power generating units like wind generators, micro-turbines, solar (PV) systems, and fuel cells, operating as an integrated and controllable system. This system is designed not only to supply electricity but also to provide heating and power services to localized areas. The rapid deployment of micro grids represents a transformative approach towards achieving energy resilience, reducing dependence on centralized power sources, and enhancing overall energy efficiency while promoting sustainable development globally [1,2]. Micro grids (MGs) are designed for flexibility, capable of operating in both on-grid and islanded modes. In on grid mode, MGs can supply power to the main utility grid during import power when necessary. The primary concern in this mode is managing power flows (real & reactive) (DGs) in and between the MG and the utility Grid(UG). Voltage and frequency control in grid-connected mode are typically handled by the larger power system, not by the MG itself. In contrast, during islanded mode, where the MG operates independently from the main grid, maintaining power balance becomes critical. In this scenario, the MG must also autonomously control its voltage and frequency to ensure stability and reliability. This dual capability of MGs—functioning seamlessly in both grid- connected and islanded modes, highlights their role in enhancing grid resilience, optimizing energy distribution, and supporting sustainable energy transitions [3, 4].

Micro grid systems with significant Distributed Generators (DGs) can experience voltage and frequency fluctuations when integrating DGs or adjusting loads. Effective MG control systems must manage these fluctuations

Journal of Information Systems Engineering and Management
2025, 10(35s)
e-ISSN: 2468-4376
https://www.jisem-journal.com/

Research Article

to avoid excessive reactive currents circulating among small sources. Even small deviations in V &f set points can result in circulating currents surpassing the capacity of the micro sources.

Figure 1 illustrates a typical MG configuration where each DG connects to the Point where all the grid components are connected (PCC) over an inverter interface. These interfaces typically employ non-linear devices like PWM Voltage Source Inverters (VSIs) or converters, facilitating DG integration within the MG or connection to the utility grid [6]. However, these devices introduce V& I disturbance due to high-frequency switching pulses, which can degrade power quality [7]. This challenge becomes pronounced as MGs integrate more DGs, highlighting significant power quality concerns [8, 9]. Addressing these issues is essential for ensuring stable and efficient working of MGs in both on-grid and islanded modes. An improved Slap Swarm Optimization (I-SSO) algorithm was used to optimize gain values for a type-II fuzzy PID controller, demonstrating its superior effectiveness compared to type-I fuzzy, PID, and PI controllers in recent implementations [10]. The PSO algorithm is integrated into PQ control mode for real-time self-tuning, ensuring balanced load sharing during load changes. The controller also monitors power flow to manage situations where load exceeds or significantly falls below the DG unit's power generation capacity [11]. Several optimization techniques have been utilized successfully to tune gain parameters of controllers, including ITAE, GA, and PSO[12,13]. These methods, although effective in damping dynamic oscillations in DGs, towards their point of common coupling (PCC), face significant challenges in micro grid operations. Micro grids operate in on or off grid modes amidst dynamic conditions such as electric vehicle (EV) loads and from sources like partially shaded photovoltaic (PV) and wind turbines (WS) experiencing varying irradiation and wind speeds. Linear ITAE- based gains often fail to ensure system stability under such vibrant deviations. Similarly, GA and PSO provides premature convergence, limiting their ability to find optimal gains under uncertain and varying conditions. Recent advancements include the Firefly algorithm (FA), which addresses multiplicity and universal search challenges through variants like harmonic search-based FA and adaptive modified firefly algorithm (AMFA) . However, these improvements introduce computational complexity that can lead to inaccurate stability assessments and suboptimal feedback paths. The (COA) [15], inspired by natural behaviour of coatis, which exhibits robust performance in highly nonlinear problems, overcoming computational complexity hurdles. To enhance micro grid stability comprehensively, this study introduces COA based PID controller, whose efficiency and performance benefits of to varying micro grid conditions. By incorporating COA, the study anticipates improved stability and performance under diverse operating scenarios typical of modern micro grid environments.

The paper starts by introducing multi-DG micro grid stability and various optimization techniques. Section 2 details the design of a multiple DG-based micro grid, outlining dynamic relationships for specific feedback paths. In Section 3, the PSO-PID technique is presented with accurate foundations tailored to meet system requirements. Section 4 evaluates the proposed optimization scheme using MATLAB scripts. A comparative analysis between COA-PID and standard PSO-PID is conducted to demonstrate COA's superiority. Finally, Section 5 offers concluding remarks and outlines future research directions.

MODEL DESCRIPTION

The Micro Grid operates with PV based DG integration and supplied from IGBT regulated voltage source converter (VSC). The MG architecture is presented in Figure-1, in which the single stage PV-DG interconnected with local load and utility Grid in parallel at point of common coupling (PCC).

Journal of Information Systems Engineering and Management
2025, 10(35s)
e-ISSN: 2468-4376
https://www.jisem-journal.com/

Research Article

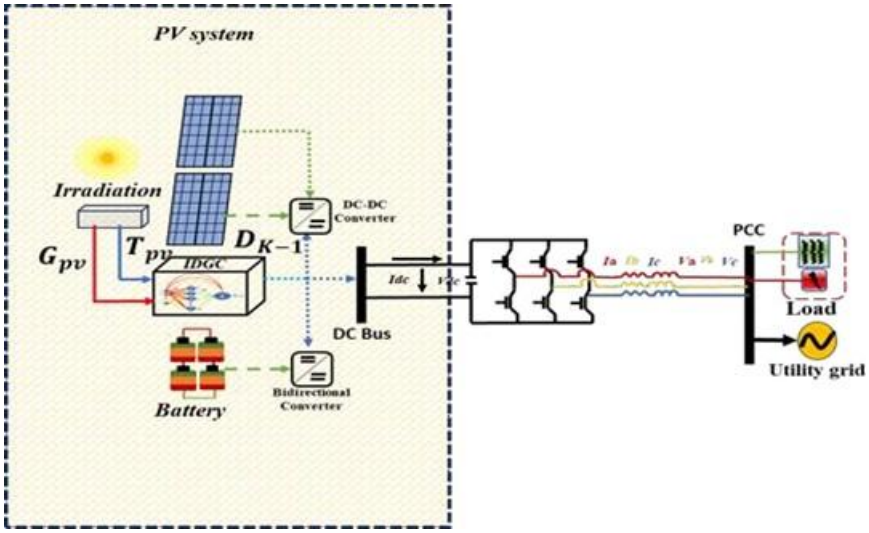

Figure 1: The Proposed Micro Grid Architecture

PV Modeling

The micro grid supplied power from PV system. The photovoltaic system consists of PV array and MPP tracker. The PV module used in this model is 40 W ELDORA-40 PV and its parametric values are listed in this section. To achieve a 400 kW PV system, a mathematical model utilizing a single diode model [12] is employed. This setup consists of 58 strings of ELDORA-40 modules, each rated at 40 W, joined in parallel. Every string comprises 15 units in series, resulting in a 33.4 kW PV group. Three of these arrays are then combined in series to reach 100 kW each. Finally, four 100 kW systems are connected in parallel to form the integrated 400 kW PV system, designed for efficient solar power generation.

Battery Modeling

This study examines the integration of a Battery Energy Storage (BES) system with solar photovoltaic (PV) technology to ensure a stable DC voltage during periods of inadequate PV generation. A 160 kW lead-acid battery, as described in reference [26], can provide up to 40% of the total PV output. At the system's start-up, the battery's State of Charge (SOC) is assumed to be at full capacity (100%). Charging and discharging functions are mathematically defined in the same reference, facilitating effective energy management between the battery and the solar system to meet power demands.

The battery current (i_{batt}) is determined by dividing the power supplied by the battery (w_{batt}) by its voltage (u_{batt}), expressed as $i_{batt} = \frac{w_{batt}}{u_{batt}}$. w_{batt} is calculated as the (W_{dcref}) and the PV power (W_{pv}), defined by Eq. (15). This setup ensures continuous and reliable power supply by managing fluctuations in solar energy output through effective battery utilization.

Figure-2 illustrates the key components of a solar PV system. A typical PV cell includes a current source, diode, and resistors organized in parallel and series configurations. These elements work together to convert solar energy into electrical power. Established formulas enable calculation of the generated current from the solar cell, supporting its vital role in renewable energy applications and technology.

Journal of Information Systems Engineering and Management
2025, 10(35s)
e-ISSN: 2468-4376
https://www.jisem-journal.com/

Research Article

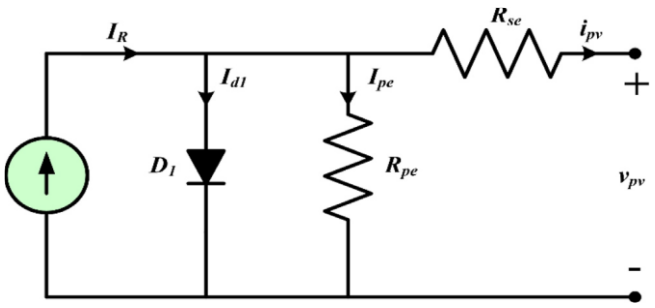

Figure 2: PV cell circuit diagram

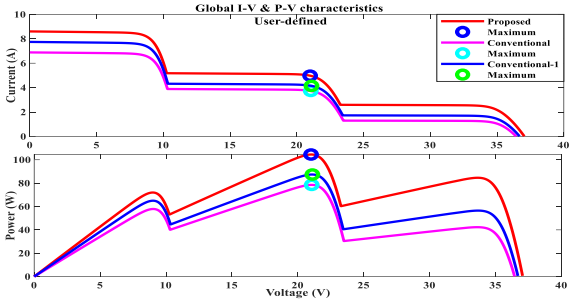

Figure 3: Multi I-V & P-V characteristics

PV output current is given by

$$i_{PV} = i_R - i_{d1} - i_{pe}$$

(1)

Here i_{PV} and v_{PV} represents the PV array output current & voltage respectively and i_R is PV cell current, i_{d1} is diode current and i_{pe} is parallel resistance current.

$$i_{d1} = i_{rs}\left(e^{\frac{q(v_{PV}+i_{PV}r_{se}}{nkT}} - 1\right)$$

(2)

Here i_{rs} represents reverse saturation current, q is electron charge, T is the cell temperature, K is Boltzmann constant and 'n' is the diode factor [14-15].

The PV cell current is expressed by

$$i_R = \frac{ir}{ir_0}\left(i_{sc} + \mu(\Gamma - \Gamma_0)\right)$$

(3)

Where i_{sc} the short circuit is current, ir is the working irradiance, ir_0 is the reference irradiance. Similarly Γ_0, is the reference temperature and μ is the cell temperature coefficient.

$$i_{PV} = i_R - i_{rs}\left(e^{\frac{q(v_{PV}+i_{PV}r_{se}}{nkT}} - 1\right) - \frac{v_{PV} + i_{PV}r_{se}}{r_{pe}}$$

4)

Here reverse saturation current is given by

Journal of Information Systems Engineering and Management
2025, 10(35s)
e-ISSN: 2468-4376
https://www.jisem-journal.com/

Research Article

$$i_{sr} = i_{srref}\left(\frac{\Gamma}{\Gamma_0}\right)^3 e^{\left[\frac{qE_g}{nK}\left(\frac{1}{\Gamma}-\frac{1}{\Gamma_0}\right)\right]} \tag{5}$$

E_g is energy band gap

A single solar cell produces 1volt to 1.5 volt which is not sufficient to supply the demand, for which the cells are connected in series or parallel or mixed grouping.

In Fig. 2, the Maximum Power Point (MPP) fluctuates due to environmental factors. Therefore, a controller is essential to optimize the PV load, aligning it as closely as feasible with the MPP.

In Fig. 2(b), the Maximum Power Point (MPP) occurs where power remains constant concerning voltage. This relationship is expressed by Equation (6).

In Fig. 2(b), the MPP is where power is constant relative to voltage. This relationship is represented by Equation (6).

$$\frac{dP}{du_{PV}} = \begin{cases} = 0, at\ MPP \\ > 0\ at\ left\ side\ of MPP \\ < 0,\ at\ right\ side\ of\ MPP \end{cases} \tag{6}$$

In a PV-based micro grid, the interrelation between Solar Photovoltaic (PV) systems and converter dynamics is crucial for efficient energy management and stability. Solar PV systems generate (DC), which needs to be converted (AC) to be compatible with the grid and local loads. The converter, or inverter, plays a pivotal role in this process by adjusting the voltage and frequency of the AC output to match the grid requirements. Effective converter dynamics ensure optimal energy conversion, minimize losses, and maintain grid stability. As solar irradiance fluctuates, the converter must adapt in real-time, balancing energy supply and demand while supporting grid resilience and reliability.

Converter Dynamics

Converter dynamics in a PV-based micro grid are essential for optimizing power flow and maintaining grid stability. The converter, or inverter, transforms (DC) to (AC) suitable for the grid. It adjusts output voltage and frequency to align with grid standards, accommodating fluctuations in solar irradiance and varying load demands. By dynamically regulating these parameters, the converter ensures efficient energy conversion and contributes to grid stability. Advanced control strategies enable the converter to respond to real-time changes, improving overall system performance and reliability within the micro grid.

VSC dynamics is written as Eq. (7)

$$\begin{bmatrix} I_{2d} \\ I_{2q} \end{bmatrix} = \frac{-R_2}{L_2}\begin{bmatrix} I_{2d} \\ I_{2q} \end{bmatrix} + \omega\begin{bmatrix} 0 & 1 \\ -1 & 0 \end{bmatrix}\begin{bmatrix} I_{2d} \\ I_{2q} \end{bmatrix} + \frac{1}{L_2}\left(\begin{bmatrix} u_{id} \\ u_{iq} \end{bmatrix} - \begin{bmatrix} u_{2d} \\ u_{2q} \end{bmatrix}\right) \tag{7}$$

This equation illuminates the relationship between the angular velocity (ω) of the d-q-frame and the converter's behavior within the system

Journal of Information Systems Engineering and Management
2025, 10(35s)
e-ISSN: 2468-4376
https://www.jisem-journal.com/

Research Article

$$u_q = \frac{i_L(1-d)L_2 + p_2 L_2 \dot{u}_{dc} + R_2 p_2 u_{dc} + X_2 Q_1 u_{dc}}{u_{dc}}$$

(8)

$$u_p = \frac{3\left(u_{id}u_{1q} - u_{iq}u_{2d}\right)}{2}$$

(9)

The second-order PLL, resembling Fig. 2, synchronizes the PV-BES system with grid. Feedback errors (ep2, eq2) for P2, Q2 are in Eq. (22). Control references are computed as shown in Eq. (23).

$$\varepsilon_{p1} = p_1^* - p_1$$
$$\varepsilon_{q1} = Q_1^* - Q_1 \quad (10)$$

$$u_{q1}^* = \left(k_{p1} + \frac{k_{i1}}{s}\right)\varepsilon_{p1} \quad (11)$$

$$u_{p1}^* = \left(k_{p2} + \frac{k_{i2}}{s}\right)\varepsilon_{q1} \quad (12)$$

$$\varepsilon(t) = \varepsilon_1(t) + \varepsilon_2(t)$$

THE PSO BASED PID

The PSO algorithm, renowned for its simplicity and efficacy, is commonly applied in fine-tuning PID controller parameters to mitigate system frequency deviations. It aims to optimize PID controller settings by orchestrating collaborative exploration within a population of particles. Each particle, treated as an individual, navigates a D-dimensional search space denoted as Xi, maintaining personal best positions P_{best}, and tracking the best global position g_{best}. With velocities v_i, particles iteratively update positions until termination criteria are met, honing in on the optimal solution and thus enhancing PID controller performance.

The velocity & position of the particles are given by

$$v_{i,d}(t+1) = w(t)v_{i,d}(t) + c_1 r_{1,d}\left(p_{besti,d} - \chi_{i,d}\right) + c_2 r_{2,d}\left(g_{best} - \chi_{i,d}\right) \quad (13)$$

$$\chi_{i,d}(t+1) = \chi_{i,d}(t) + v_{i,d}(t+1) \quad (14)$$

$$w(t) = w_{\max} - \left(\frac{w_{\max} - w_{\min}}{\max iter}\right) \times iter \quad (15)$$

The PID controller parameters are optimized by PSO by minimizing system deviations. $\chi_{i,d}$ & $v_{i,d}$ are the position and velocity vectors.The inertia weight (w), perceptive and societal parameters ($c1$ and $c2$), and arbitrary numbers ($r1$ and $r2$) lies in [0, 1]. $p_{besti,d}$ and $g_{best,d}$ are the best personal & global.

Journal of Information Systems Engineering and Management
2025, 10(35s)
e-ISSN: 2468-4376
https://www.jisem-journal.com/

Research Article

COATI OPTIMIZATION TECHNIQUE

The Coati Optimization Technique is an advanced algorithm inspired by the foraging behavior of coatis, a group of mammals known for their cooperative hunting strategies. This technique leverages the coati's method of resource searching and problem-solving to address complex optimization challenges. By mimicking the way coatis explore their environment and work together to find food, the algorithm effectively navigates the search space to identify optimal solutions. It balances exploration and exploitation through a collaborative approach, enhancing convergence speed and solution quality in various optimization problems. This technique is particularly useful in fields like engineering and data science, where efficient and accurate solutions are crucial.

Inspiration and Behaviours of Coatis

The COA is inspired by the behaviours and strategies of coatis, mammals from the south-western United States, Mexico, Central America, and South America. Recognizable by their slim heads, flexible noses, black paws, small ears, and long, non-prehensile tails, coatis are about the size of a large house cat, measuring between 33 and 69 cm in length and weighing 2 to 8 kg. Males are generally larger than females and have more pronounced canine teeth. Coatis are omnivorous, consuming a range of invertebrates and small vertebrates, including green iguanas, which they hunt using coordinated group tactics. Their hunting and evasion strategies against predators like jaguars, ocelots, and large birds of prey inspire the COA. This algorithm replicates coatis' cooperative hunting and strategic evasion to solve complex optimization problems, reflecting their adaptability and strategic problem-solving abilities.

Initialization

The Coati Optimization Algorithm (COA) is a population-based metaheuristic where each coati represents a candidate solution in the search space. The coatis' positions correspond to the decision variable values. Initially, these positions are randomly assigned across the search space according to Eq. (1). This setup allows the COA to explore and optimize solutions iteratively, with each coati's movement reflecting the algorithm's search for optimal results.

$$\chi_i = \chi_{i,j} = l_{bound,j} + r.\left(u_{bound,i} - l_{bound,j}\right) \text{ Where } i = 1,2,3,.....N, \quad j = 1,2,.....m \tag{16}$$

In the Coati Optimization Algorithm (COA), the position $\chi_{i,}$ of the i_{th} coati represents its location in the search space $\chi_{i,j,}$. Each denotes the value of the j_{th} decision variable. With N coatis and m decision variables, r is a random real number between [0, 1], and l_{bound} and u_{bound} are the respective lower and upper bounds for each decision variable j .

The population matrix is given by

$$\chi = \begin{bmatrix} \chi_1 \\ \vdots \\ \chi_i \\ \vdots \\ \chi_{N,1} \end{bmatrix} = \begin{bmatrix} \chi_{11} & \cdots & \chi_{1j} & \cdots & \chi_{1m} \\ \vdots & \ddots & \vdots & \ddots & \vdots \\ \chi_{i1} & \cdots & \chi_{i,j} & \vdots & \chi_{im} \\ \vdots & \ddots & \vdots & \ddots & \vdots \\ \chi_{N1} & \cdots & \chi_{N.j} & \cdots & \chi_{Nm} \end{bmatrix}_{N\times m} \tag{17}$$

Evaluating candidate solutions through their positions in the decision variables yields different values for the problem's objective function. These values are determined using Eq. (3).

$$F = \begin{bmatrix} F_1 \\ \vdots \\ F_i \\ \vdots \\ F_i \end{bmatrix} = \begin{bmatrix} F(\chi_1) \\ \vdots \\ F(\chi_i) \\ \vdots \\ F(\chi_N) \end{bmatrix} \tag{18}$$

Journal of Information Systems Engineering and Management
2025, 10(35s)
e-ISSN: 2468-4376
https://www.jisem-journal.com/

Research Article

Let F represent the vector of objective function values, with F_i being the value derived from the i_{th} coati's performance.

In met heuristic algorithms like the proposed COA, a candidate solution's quality is determined by its objective function value. Consequently, the individual in the population that achieves the optimal objective function value is considered the best. As the algorithm iterates and candidate solutions are refined, this top-performing member is continually updated. Each iteration evaluates and possibly replaces the best member, ensuring that the population's overall quality improves throughout the optimization process [15].

Modelling of COA

The updating method of coatis depends on coati's behaviour, which includes Coati's approach during attacking iguanas and escaping from pre daters. Thus the population is updated in two different phases.

Exploration Phase

The initial phase of updating the coatis' positions within the search space is modelled after their hunting strategy for iguanas. In this method, some coatis climb a tree to scare the iguana, while others wait below for it to fall. Once the iguana is on the ground, the coatis attack and capture it. This tactic illustrates the COA's capability for exploration in the global search space. In COA, the best member's position represents the iguana's location. Half of the coatis climb the tree, while the other half wait below, with their positions mathematically simulated by Eq. (4). This strategy enhances the algorithm's exploration efficiency.

$$\chi_{i,j}^{p_1} : \chi_{i,j} + r\left(I_{guanaj} - I.\chi_{i,j}\right) \quad for \; i = 1,2,3,.....\frac{n}{2}, \quad j = 1,2,....m \tag{19}$$

After the iguana falls, it is randomly positioned within the search space. The ground coatis then move based on this new position, which is modelled using Equation (5) and (6).

$$I_{guana}^{G} : I_{guanaj}^{G} = l_{boundj} + r\left(u_{boundj} - l_{boundj}\right), \; j = 1,2,3.....m \tag{20}$$

$$\chi_i^{p1} : \chi_{i,j}^{p1} = \begin{cases} \chi_{i,j} + r.\left(I_{guanaj}^{G} - I.\chi_{i,j}\right), F_{IguanaG} < F_i \\ \chi_{i,j} + r\left(\chi_{i,j} - I_{guanaj}^{G}\right) else \end{cases} \tag{21}$$

Coatis accept new positions if they enhance the objective function's value; otherwise, they retain their current positions, as per the update condition in Equation (7) for iterations 1 to n. This update condition is simulated using following equation.

$$\chi_i = \begin{cases} \chi_i^{p1} & F_i^{p1} < F_i \\ \chi_i & \end{cases} \tag{22}$$

The new position χ_i^{p1} for the i_{th} coati is calculated based on its j_{th} dimension. If the resulting objective function value F_i^{p1} improves, the coati adopts this position. Randomness, represented by r, I, and Iguana, introduces variability into the optimization process.

Exploration Phase

The next stage in updating coati positions mimics their natural response to predators, emphasizing both escape and local exploration. Coatis strategically manoeuvre to safety, staying near their current position. This process reflects their ability to exploit local areas effectively. Fig. 3 illustrates the pattern of coati behaviour when evading

Journal of Information Systems Engineering and Management
2025, 10(35s)
e-ISSN: 2468-4376
https://www.jisem-journal.com/

Research Article

predators, guiding the algorithm's optimization strategy.

For simulation the following equation may be used.

$$l_{boundj}^{local} = \frac{l_{boundj}}{t} \qquad u_{boundj}^{local} = \frac{u_{boundj}}{t} \tag{23}$$

$$\chi_i^{p2} : \chi_{i.j}^{p2} = \chi_{i,j} + (1-2r).\left\{ l_{boundj}^{local} + r.\left(u_{boundj}^{local} - l_{boundj}^{local} \right) \right\} \tag{24}$$

$i = 1,2,3....n \quad j = 1,2,3,.....m$

If the new position enhances the objective function value, it's deemed acceptable, as per Equation (10).

$$\chi_i = \begin{cases} \chi_i^{p2} & F_i^{p2} < F_i \\ \chi_i & else \end{cases} \tag{25}$$

χ_i^{p2} Represents the new position for the i_{th} coati, determined in the second phase of COA. $\chi_{i,j}^{p2}$ denotes its j_{th} dimension. F_i^{p2} is the objective function value, r is a random number. t signifies the iteration count. l_{boundj}^{local} and u_{boundj}^{local} are local bounds for dimension j, while l_{boundj} and u_{bound} are global bounds.

Coati Optimization Algorithm

1. Arrange the information's of optimization problems.
2. Set the iteration count'Γ' and number of coatis 'm'.
3. Position of coatis are initialized, objective function is evaluated with this initial population.
4. *for* $t = 1 : \Gamma$
5. Find the best location of iguana with best number of population's location.
6. **Exploration Phase (hunting and attacking the iguana)**
7. For i=1:m/2
8. From equation (4) new coatis positions can be calculated.
9. Update the i_{th} coati position from equation (7)
10. **End**
11. *for* $i = 1 : m/2 : m$
12. The arbitrary iguana position can be calculated from equation (5)
13. New position of i_{th} coati can be calculated, from equation (6)
14. Update the coati position using equation (7)
15. **End for**
16. **Exploation Phase (method of escaping from Predator)**
17. Find the local bound of the variables using equation (8)
18. **For i=1:m**
19. Find coatis fresh position, using equation (9)
20. Update the coatis position using equation (10)
21. **End**

Journal of Information Systems Engineering and Management
2025, 10(35s)
e-ISSN: 2468-4376
https://www.jisem-journal.com/

Research Article

22. Save the best candidate found so far
23. End
24. Output for the Coati optimized problem can be achieved.
25. End COA

The objective function is

$$F = ISE = \int_0^t (\varepsilon(t))^2 dt \qquad (26)$$

Where ε is the error in frequency, t is the simulation time.

F is the objective function subjected to constraint

$$K_{p\min} \leq K_p \leq K_{P\max}$$

$$K_{I\min} \leq K_I \leq K_{I\max} \qquad (27)$$

$$K_{D\min} \leq K_D \leq K_{D\max}$$

RESULT ANALYSIS

In this study, the Grey Wolf Optimizer Algorithm (GOA) was employed to determine the optimal parameters of PI and D controllers in an Islanded Micro grid (MG) system. The objective was to minimize a predefined function, and subsequent results were compared with controllers optimized using Particle Swarm Optimization (PSO) under identical operating conditions. The three-phase grid-connected Voltage Source Inverter (VSI) system and its controller were modelled using MATLAB/Simulink version 2017a. PSO algorithms were implemented in MATLAB to minimize the objective function, with 50 particles and iterations set for fair comparison. The parameter optimization involved defining search spaces through a trial and error method, varying from 0 to 50. Each of the two solar PV modules utilized had a power rating of 50 kW. Simulations were conducted at a sampling frequency of 500 kHz, corresponding to a sampling time of 2 microseconds. Key model parameters included a line inductance of 6 mH, operating frequency of 50 Hz, and DG units rated at 50 kW each. The current control parameters for PWM-based controllers were established as $k_p = 11.823, k_i = 0.00318, k_d = 6.332$ by the proposed COA-PID controller. The switching frequency for PWM was fixed at 10 kHz, synchronized with a sampling frequency of 500 kHz. Performance evaluations of the proposed controllers were conducted across three distinct case studies, providing insights into their effectiveness compared to PSO-optimized counterparts.

Scenario-1: Three Phase Fault at PCC

In evaluating system performance under fault conditions at the Point of Common Coupling (PCC), the effectiveness of an innovative control strategy becomes evident. When a fifty-cycle three-phase fault is introduced at t = 1s, the new control technique rapidly stabilizes the system, attenuating oscillations within just 2 seconds or 100 cycles. This is a significant improvement over traditional methods, which take approximately 5 seconds or 200 cycles to restore system stability. The proposed COA-PID control, as depicted in Figure -4, ensures stable PCC voltage between the utility and distributed generation (DG) sources (Figure -1). The cost function convergence is achieved swiftly, within 20 iterations, with optimally tuned parameters. Simulations of PCC current, and real and reactive power during the fault period (1 to 1.2 seconds) reveal the COA-PID's superior performance compared to conventional PID and PSO-PID controllers. The WOA-PID technique excels in reducing overshoot and settling time, making it a robust solution for enhancing grid stability and operational efficiency under fault conditions.

Journal of Information Systems Engineering and Management
2025, 10(35s)
e-ISSN: 2468-4376
https://www.jisem-journal.com/

Research Article

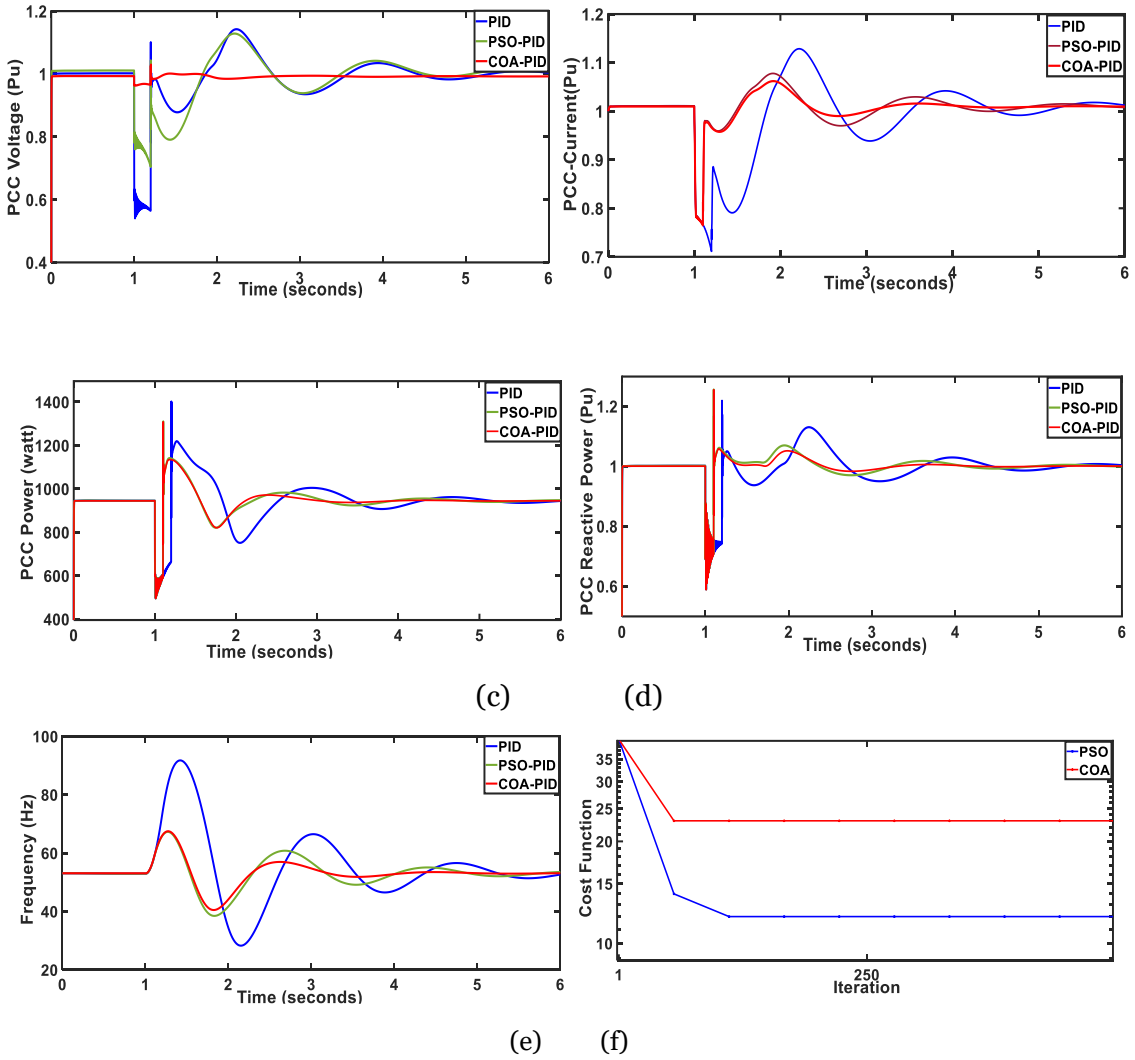

Figure 4: Performance of the controller during three phase fault at PCC (a) PCC voltage, (b) PCC current (c) Real power at PCC (d) Reactive power at PCC (e) PCC frequency (f) Convergence of the optimization techniques.

Scenario 2: Partial Shading

Optimal power output from a Multi-Panel Photovoltaic System (MPVS) relies heavily on the arrangement of PV panels in series and parallel configurations. Series connections increase the output voltage, while parallel connections boost the output current, which is essential for accurately modelling the PV array's current-voltage (I-V) characteristics. The single diode model, often preferred for its simplicity and lower computational needs, effectively simulates the effects of partial shading, which create multiple peaks in the PV array's power-voltage (P-V) curves, as shown in Figure-7 (a & b). During partial shading, such as when individual cells are disconnected, the PV array displays distinct peaks: a global maximum (GM) and several local maxima (LM), reflecting varying irradiance levels. For example, a 100-watt PV panel with 60 cells (40 in series and 20 in parallel) demonstrates these peaks under non-uniform irradiation. The disturbances caused by shading impact the Micro Grid System, leading to fluctuations in PCC voltage (about 2.5 Pu) and current (0.4 Pu). The proposed COA-PID controller effectively minimizes these deviations more quickly than traditional methods, enhancing stability and efficiency. Accurate modelling and control under partial shading are critical for optimizing power generation and grid stability.

Journal of Information Systems Engineering and Management
2025, 10(35s)
e-ISSN: 2468-4376
https://www.jisem-journal.com/

Research Article

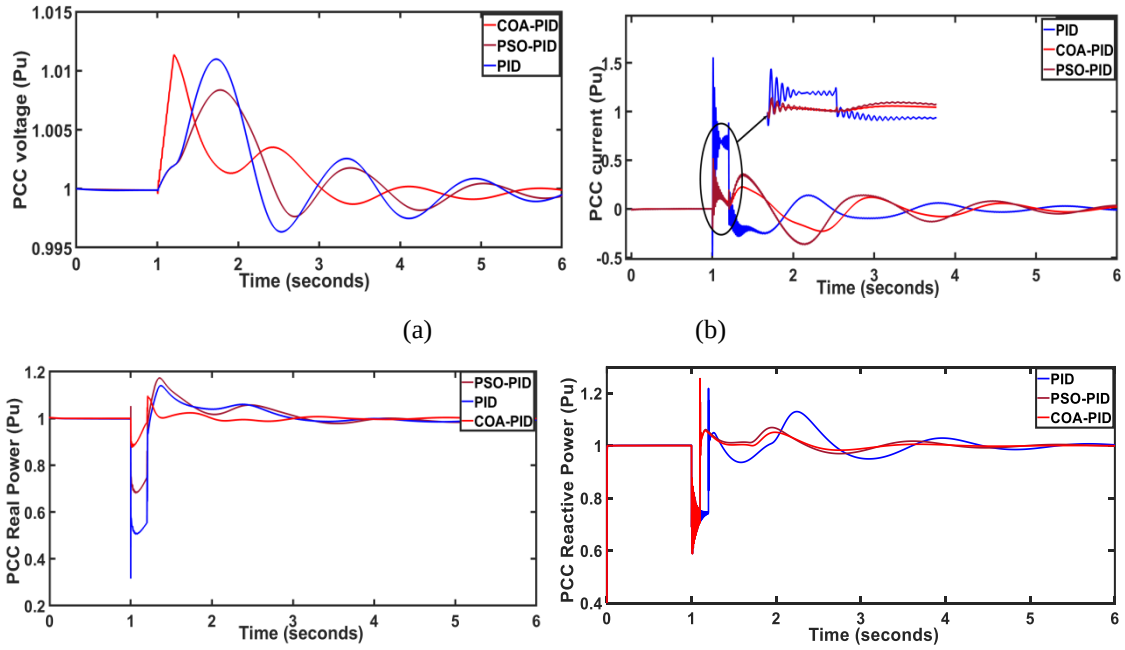

Figure 5: Performance of the controller during Partial Shading (a) PCC voltage, (b) PCC current (c) Real power at PCC (d) Reactive power at PCC.

Scenario 3: Battery Parameters during System Uncertainties

Figure 8(b) demonstrates the smooth transition of a PV-battery system from standalone to grid-connected mode at 0.5 seconds into the simulation, which lasts for 1 second. The performance of PID and PSO-PID controllers is similar, so Figure -5, compares PID with COA-PID. During the transition, the Boost current remains steady, ensuring optimal PV array performance. In grid-connected mode, surplus power is fed back to the grid, and battery current approaches zero due to a zero command from the battery controller. The system maintains stable sinusoidal grid currents with no observable fluctuations in current or power waveforms. The COA-PID controller achieves a steady state within 0.1 seconds (5 cycles), demonstrating effective performance during mode changes.

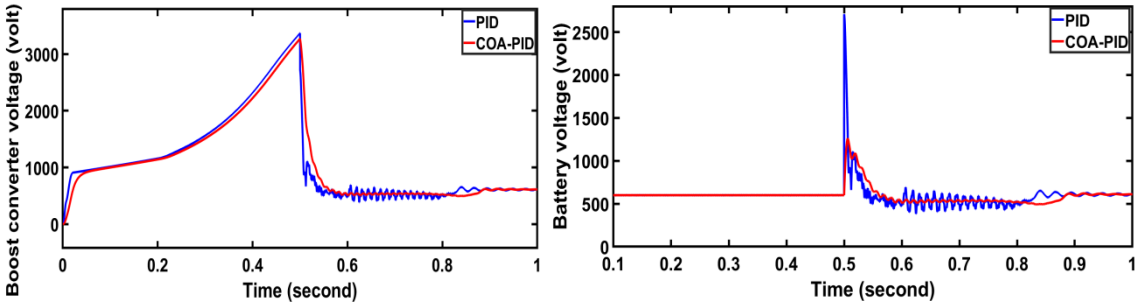

Journal of Information Systems Engineering and Management
2025, 10(35s)
e-ISSN: 2468-4376
https://www.jisem-journal.com/

Research Article

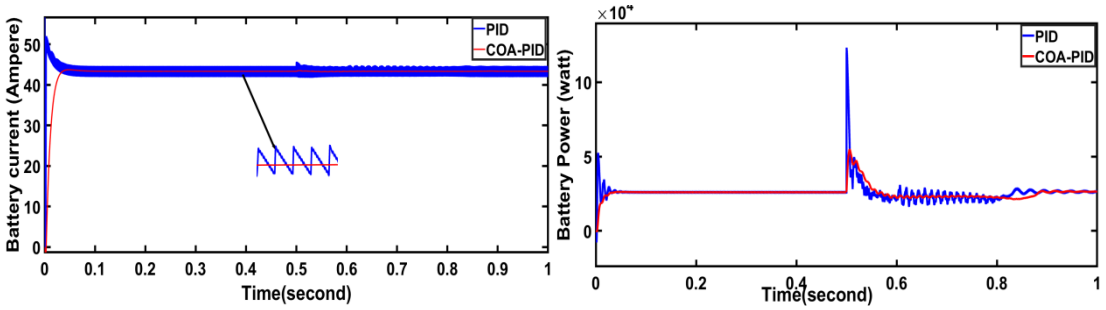

(c) (d)

Figure-6: Performance of the controller through shifting from isolated to on grid operation(a) Boost Converter voltage, (b) Battery Voltage (c) Battery current (d) Battery real Power.

CONCLUSION

This study advances micro grid performance through a novel COA-based PID controller. Utilizing WOA-based optimization, the approach aims to minimize parametric errors in micro grid dynamics, integrating PV system parameters across various DGs. The WOA-PID controller, with its sinusoidal characteristics, excels under varying solar and grid uncertainties. Extensive analysis of grid parameters reveals reduced transient oscillations due to COA-optimized control gains. Evaluations of micro grid stability through damping factor calculations show notable improvements. Comparative studies demonstrate that the COA technique reduces system restoration time, proving its effectiveness and rapid convergence in optimizing system responses. Looking ahead, COA optimization can enhance coordination scheduling, improve battery management, and contribute to more efficient energy systems, making it a key tool for advancing micro grid stability and performance.

Acknowledgement

This research is funded by Universiti Teknologi MARA under the Special Research Grant [Geran Penyelidikan Khas 600-RMC/GPK 5/3 (129/2020)]. Authors would also like to acknowledge College of Engineering, UiTM for the excellent facility provided to carry out this research.

REFERENCES

[1] Lasseter, R.H. Microgrids. In Proceedings of the Power Engineering Society Winter Meeting, New York, NY, USA, 27–31 January 2002; pp. 305–308.
[2] Ghanbari, N.; Bhattacharya, S.; Mobarrez, M. Modeling and Stability Analysis of a DC Microgrid Emp loyingDistributed Control Algorithm. In Proceedings of the 2018 9th IEEE International Symposium on Power Electronics for Distributed Generation Systems (PEDG), Charlotte, NC, USA, 25–28 June 2018; pp. 7.
[3] Al-Saedi,W.; Lachowicz, S.W.; Habibi, D.; Bass, O. Voltage and frequency regulation based DG unit in an auto nomous microgrid operation using Particle Swarm Optimization. Int. J. Electr. Power Energy Syst. 2013, vol 53, PP.742–751.
[4] Olivares, D.E.; Mehrizi-Sani, A.; Etemadi, A.H.; Cañizares, C.A.; Iravani, R.; Kazerani, M.; Hajimiragha, A.H., Gomis-Bellmunt, O.; Saeedifard, M.; Palma-Behnke, R. Trends in microgrid control. IEEE Trans. Smart Grid 2014, Vol.5, 1905–1919.
[5] Piagi, P.; Lasseter, R.H. Autonomous control of microgrids. In Proceedings of the Power Engineering Society General Meeting, Montreal, QC, Canada, 8–22 June 2006; p. 8.
[6] Nejabatkhah, F.; Li, Y.W. Overview of power management strategies of hybrid AC/DC microgrid. IEEE Trans. Power Electron. 2015, vol.30, PP.7072–7089.
[7] Zeng, Z.; Yang, H.; Zhao, R.; Cheng, C. Topologies and control strategies of multi-functional grid-connected inverters for power quality enhancement: A comprehensive review. Renew. Sustain. Energy Rev. 2013, vol.24, PP.223–270.
[8] Görbe, P.; Magyar, A.; Hangos, K.M. Reduction of power losses with smart grids fuelled with renewable sources and applying EV batteries. J. Clean. Prod. 2012, vol.34, 125–137.
[9] Jiayi, H.; Chuanwen, J.; Rong, X. A review on distributed energy resources and MicroGrid. Renew. Sustain. Energy Rev. 2008, vol.12, PP.2472–2483.

Research Article

[10] Prakash Chandra Sahu ∗ , Sonalika Mishra, Ramesh Chandra Prusty, Sidhartha Panda, 'Improved-salp swarm optimized type-II fuzzy controller in load frequency control of multi area islanded AC micro grid ' Sustainable Energy, Grids and Networks , Elsevier, Volume 16, December 2018, Pages 380-392.

[11] Waleed Al-Saedi, Stefan W. Lachowicz, Daryoush Habibi, Octavian Bass, 'Power flow control in grid-connected micro grid operation using Particle Swarm Optimization under variable load conditions ' International Journal of Electrical Power & Energy Systems, Elsevier, Volume 49, July 2013, Pages 76-85.

[12] Wang S-C, Liu Y-H (2014) A PSO-based fuzzy-controlled searching for the optimal charge pattern of Li-ion batteries. IEEE Trans Indu Electron, vol. 62, No.5, PP.2983–2993.

[13] Panda S, Padhy NP, Patel RN (2008) Power-system stability improvement by PSO optimized SSSC-based damping controller.Electr Power Compon Syst 36(5):468–490.

[14] Mohammadi S, Mozafari B, Solimani S, Niknam T (2013) An adaptive modified firefly optimisation algorithm based on hong's point estimate method to optimal operation management in a microgrid with consideration of uncertainties. Energy, vol.51, PP.339–348.

[15] Mohammad Dehghani , Zeinab Montazeri , Eva Trojovská , Pavel Trojovský, 'Coati Optimization Algorithm: A new bio-inspired metaheuristic algorithm for solving optimization problems ' Knowledge-Based Systems, Elsevier, Vol. 259, 2023, PP. 1-43.